Structural Evolution of Poly(lactic acid)/Poly(ethylene oxide)/Unmodified Clay upon Ambient Ageing

Joffrey Derho, Jérémie Soulestin, Patricia Krawczak

Mines Douai, Department of Polymers and Composites Technology and Mechanical Engineering, 941 rue Charles Bourseul, CS 10838, F-59508 Douai, France

Correspondence to: J. Soulestin (E-mail: jeremie.soulestin@mines-douai.fr)

ABSTRACT: Poly(lactic acid) (PLA) and poly(ethylene oxide) (PEO)/unmodified clay masterbatches are compounded together in order to investigate the ambient ageing of the resulting PLA/PEO/clay ternary blends. Binary blends are miscible up to 20 wt PEO% and in ternary counterparts, clay is intercalated at a nanometric scale, similarly to the clay dispersion state in masterbatches. PEO/clay interactions are strong, as confirmed by the lower plasticization of ternary blends. Furthermore, structural modifications occurring over time are evidenced for all blends through the observation of changes in thermal responses. Over the 220-day observation period, lower plasticized samples undergo physical ageing only whereas blends close to the miscibility limit know a rapid PLA/PEO phase separation without physical ageing. For blends with intermediate PEO concentrations, both phenomena are observed with slower PLA chain mobility transition. Remarkably clay appears to affect both phenomena, ternary blends having limited physical ageing and slower PLA/PEO segregation. © 2014 Wiley Periodicals, Inc. J. Appl. Polym. Sci. **2014**, *131*, 40426.

INTRODUCTION

Obtaining poly(lactic acid) (PLA) compounds with balanced functional properties often motivates the combined use of plasticizer and nanofillers to produce ternary blends with improved properties compared to the neat polymer. In particular, numerous studies aim at improving the ductility of PLA without compromising its stiffness.[1–4] In addition, simultaneous improvement of other functional properties like barrier properties,[5,6] thermal stability[6] or transparency[7] explain that these compounds are mainly interesting for flexible packaging, including food product packaging.[6,8–10] Besides, plasticizers are also likely to improve the dispersion of nanoclay during the nanocomposite manufacturing process, because of their ability to increase the matrix chains mobility[1,3,11] and their capacity to intercalate the nanolayers or cointercalate jointly with the chains of the matrix.[12] Various plasticizers were used up to now to elaborate plasticized PLA-based nanocomposites, including poly(ethylene glycol) (PEG) also called poly(ethylene oxide) (PEO) for homopolymers with longer chains,[13–16] poly(ethylene glycol-co-propylene glycol) (PEPG),[13] polyadipates,[17,18] or oligomeric lactic acid (OLA).[19]

A crucial requirement to properly choose the plasticizer-matrix pair is its stability over time.[13,17] The permanence of plasticized

PLA-based compounds structure, morphology and set of properties remains a challenge,[20] as neat PLA itself undergoes physical ageing after being processed. This originates from chains rearrangements taking place over time. After quenching, PLA amorphous phase is thermodynamically uns\. Thus, the structure of amorphous phase is likely to rearrange, due to the relative vicinity of the storage temperature (T_S) and the glass transition temperature (T_g). In these conditions, amorphous chains mobility is sufficient to enable short-distance rearrangements with time, naturally leading to the formation of locally ordered domains. As a result these local morphology modifications can induce significant properties changes, such as embrittlement or permeability drop of the materials.[19,21,22] For binary blends, several PLA-plasticizer associations were found to be unstable over time.[13–19,23–27] Several studies point out that the significance and the type of ageing mechanisms actually depend on the resulting T_g of the binary blend and its relative closeness to T_S.[13–19]

These studies distinguish two main schemes. On one hand, when the T_g of the PLA/plasticizer blend is higher than T_S (i.e., for moderately plasticized materials), ageing may take place relatively slowly over the storage time and through the physical ageing phenomenon described above. The local PLA chain

rearrangements in the amorphous phase generate a decrease in the free volume and a certain degree of phase segregation between PLA and plasticizers. As a result, effects of plasticization on material properties are partially or fully lost, ductility drop and barrier properties increase being the main consequences.[13,16–19] In particular Martino et al studied the ambient ageing of PLA/polyadipate blends over 2 months, showing that PLA chain ordering takes place in the amorphous phase over the period. In addition, no cold-crystallization was detected during the ageing. Furthermore, a light embrittlement of the most plasticized materials was noticed.[18]

On the other hand, when the binary T_g is equal to or lower than T_S (i.e., for more plasticized materials), ageing effects generally occur more rapidly and are more significant.[13,16] Furthermore, the occurrence of cold-crystallization phenomena during the storage time appears predominant. For several plasticized PLA blends having their T_g initially close to or below T_S, cold-crystallization of PLA chains actually causes the phase separation characterized by a partial loss of the plasticization effects.[13,14,17,19] Remarkably, Pluta et al. highlighted that the PLA cold-crystallization identified upon ageing of a PLA/20%PEG blend is linked to chain scissions. The measured $\overline{M_n}$ values for PLA significantly decrease over a 4-year period. This was ascribed to hydrolytic degradation of PLA chains. Cold-crystallization of PLA in turn induces phase separation, characterized by the deplasticization of PLA chains and a migration of PEG chains to the surface.[14] Contrary to the latter studies, Hu et al. correlated PEG cold-crystallization and mechanical properties variations over ageing time in the case of a high-stereo regularity PLA/20%PEG blend. In that case, PEG cold-crystallization is the driving force for PLA matrix deplasticization and embrittlement. For a quenched PLA/30%PEG blend, a spontaneous phase separation mechanism occurs in <48 h. But in the case of the same blend left in a semi-crystalline state from a slower cooling, atomic force microscopy reveals a concomitant PEG epitaxial cold-crystallization around spherulites which is assumed to deplete surrounding regions in PEG until these ones become glassy—i.e. until $T_g = T_S$ locally.[15,16]

Few studies were undertaken about the ageing of PLA-based plasticized nanocomposites.[14,18,28] Some authors have found that well dispersed nanoclays could limit or slow down the ageing of the plasticized blends.[14,18] Pluta et al. first studied the influence of clays on the ageing of a PLA/PEG blend. The presence of platelets in the matrix slows down the hydrolytic degradation brought out for the binary blends. This retarding effect is more pronounced when PLA/organoclay affinity is higher.[14] Similarly Martino et al. established that dispersed clay limits the ageing of PLA/polyadipate/organo-modified montmorillonite ternary blends. PLA chain reaccomodations may actually be hindered thanks to clay-polymer chains interactions.[18] Accordingly, Ozkoc et al. also focused on long-term ageing of PLA/PEG/organoclay materials. In such systems, chain rearrangements occurring over 1-year storage are such that PEG plasticization effects on PLA are dramatically lost. In addition, the partially exfoliated structures obtained before ageing turn into intercalated/tactoidal morphologies. These

modifications were attributed to phase separation mechanisms occurring in the matrix with time, including PEG chains out-diffusion which could be the reason why platelets reaggregate.[28]

To our better knowledge, the ageing of PLA/PEO/unmodified clay ternary blends has never been investigated in detail. It can be argued that PLA has a very poor affinity with unmodified clay, PLA being rather hydrophobic.[29] Indeed melt-blending of the two constituents resulted in microcomposites with no chain intercalations in two separate studies.[4,12] On the other hand, PEO has a high affinity with native clay, this originating from the hydrophilic character of the polyether. Interestingly, Vaia et al. prepared highly intercalated PEO/natural montmorillonite nanocomposites by simple static annealing.[30] Therefore, the high affinity between PEO and unmodified clay combined with the potential miscibility of PEO with PLA appear as a promising method to elaborate PLA-based ternary blends with tailored properties, including unique ageing behavior. This is the topic of the present work. The use of intermediate PEO/clay masterbatches to process the blends also constitutes an original aspect of the study.

EXPERIMENTAL

Materials
The PLA used is a grade having a L-lactide ratio of 98% (PLA4032D, Natureworks). The PEO chosen has an average molecular weight of 100,000 g mol^{-1} (POLYOX WSR N-10, DOW). The clay is an unmodified sodium montmorillonite (MMT) (Cloisite®Na+, Southern Clay, USA).

Samples Preparation
PLA/PEO/unmodified clay ternary systems were compounded using a two-extrusion process. PEO and clay were first melt-blended, and then the resulting PEO/clay masterbatches were diluted into PLA. Both extrusions were carried out in a twin-screw extruder (Haake Polylab, Thermo Scientific, Germany) equipped with a 16 mm diameter screw having a length/diameter ratio L/D of 40 : 1. The first extrusion step was carried out with a temperature profile gradually increasing from 80 to 110°C and a rotation speed of 150 rpm while, for the second step, the extruder was operated using a temperature profile ranging from 170 to 190°C and a rotation speed of 100 rpm. Masterbatches with different PEO/clay ratios were initially melt-blended in order to produce ternary blends ("ternaries") with specific PEO and clay weight fractions. Compositions of resulting PLA-based binary and ternary blends and PEO/clay masterbatches are presented in Table I. PEO fraction is defined as the PEO/polymer ratio and named x whereas clay concentration named y is the filler loading in the whole material. Also, for comparison purpose, binary blends PLA/PEO ("binaries") taken as references were processed from PEO extruded alone in the same conditions as PEO/clay masterbatches. Binary and ternary blends are named PLAxPEO and PLAxPEOyMMT, respectively. Finally, all compounds were injection-molded (Babyplast 6/10P, Cronoplast, Abrera, Spain) using the temperature profile 180-180-190°C (from hopper to nozzle) and finally stored under controlled conditions (23°C and 50% humidity).

Table I. Compositions of PEO/Clay Masterbatches (MB) and PLA/PEO and PLA/PEO/Clay Blends

Samples designation	PLA/polymer (wt %)	PEO/polymer (wt %) (x)	Clay wt % in MB	Clay wt % in blend (y)
PLA	100	0	n.a.	0
PLA10PEO	90	10	0	0
PLA10PEO3MMT	90	10	24	3
PLA15PEO	85	15	0	0
PLA15PEO3MMT	85	15	17.5	3
PLA20PEO	80	20	0	0
PLA20PEO3MMT	80	20	13.8	3

Figure 1. DSC traces of "0-day" PLA and PEO samples.

Characterization Techniques

Differential Scanning Calorimetry (DSC). DSC measurements were performed from −70°C to 200°C at a heating rate of 10°C/min under nitrogen atmosphere (Perkin Elmer, DSC 8500, USA). "Day 0" samples were obtained by heating the injection-molded sample for 1 min at 200°C, i.e., above melting temperature before a fast cooling to erase ageing effects. The glass transition, cold crystallization and melting temperature values obtained from DSC curves are noted "$T_{g\ DSC}$," "T_c" and "T_m," respectively. Fox Equation is used to calculate the theoretical T_g values of miscible PLA/PEO blends [eq. (1)].[16]

$$\frac{1}{T_g} = \frac{\omega_{PLA}}{T_{gPLA}} + \frac{\omega_{PEO}}{T_{gPEO}} \quad (1)$$

where ω_{PLA} and ω_{PEO} are the weight fractions of PLA and PEO, respectively. Crystallinity rate (X_c) of PLA is calculated from cold-crystallization and melting enthalpy values (ΔH_c and ΔH_f, respectively, algebraic values) according to eq. (2):

$$X_c = \frac{\Delta H_c + \Delta H_f}{\omega_{PLA} \times \Delta H_{f0}} \quad (2)$$

where ΔH_{f0} is the enthalpy value of a PLA crystal (94 J g^{-1}).[14] Besides the enthalpy value corresponding to the exothermic peak preceding the melting peak in the case of the blends is written $\Delta H_{\alpha'-\alpha}$, this exothermic peak being characteristic of PLA chains reordering from crystalline phase α' to crystalline phase α as commonly known.[17,19]

Dynamic Mechanical Analysis (DMA). DMA was carried out in tensile mode, from −70 to 130°C, at a heating rate of 3°C min^{-1} and a constant frequency of 1 Hz (Acoem, Metravib DMA+150, France). The temperature value corresponding to tan(δ) loss factor maximum is written "$T_{g\ DMA}$."

X-ray Diffraction (XRD). XRD characterization of the structure was performed on clay powder or injection-molded disks. Wide-angle X-ray scattering experiments were carried out at room temperature in reflection mode. XRD patterns were recorded on a diffractometer (D5000, Siemens, Germany) operating at 40 kV and 30 mA with a beam consisting of Co Kα radiation (λ = 1.78897 Å).
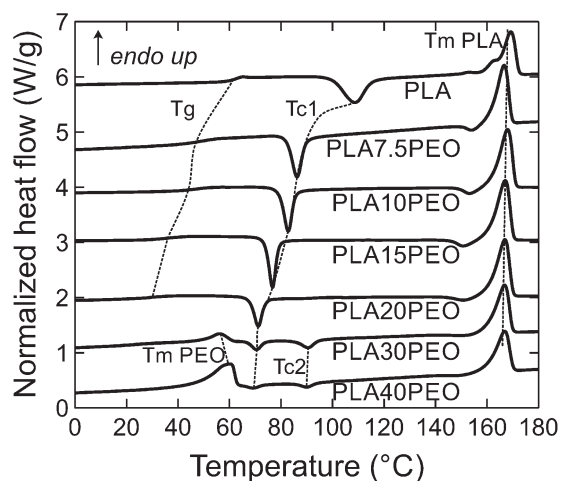
RESULTS AND DISCUSSION

Miscibility and Crystallization Ability of PLA/PEO Blends
DSC traces related to 0-day binary PLA/PEO blends are shown in Figure 1. For samples containing 20 wt % PEO or less, single T_g and T_c appear and their values both significantly decrease as the PEO concentration increases. To a lesser extent, T_m also diminishes in the PLA/PEO blends compared to PLA (see also Table II). Moreover, the evolution of T_g vs. PEO concentration follows the theoretical evolution given by the Fox equation (Figure 2). This observation tends to prove that the plasticization potential of PEO on PLA is entirely achieved and hence, that PEO is fully miscible with PLA in the resulting blends up to 20 wt %. Besides, the monotonous decrease of the binaries' T_g with PEO content is also confirmed by the DMA measurements of samples aged for 5 days. $T_{g\ DMA}$ reaches a minimum for the PLA20PEO sample. Increasing PEO proportion above 20 wt % does not result in further decrease (Figure 2).

The XRD diffractograms obtained for PLA and PLA/PEO blends are gathered in Figure 3. Blends exhibit the typical amorphous halo up to 10 wt % PEO, whereas a single peak is detected at around 19° (d = 5.4 Å) for PLA15PEO and PLA20PEO blends. According to several authors, this peak is characteristic of the PLA α-crystallographic form.[13,17,19] Along with the DSC results (Table II), it confirms that PEO plasticization increases the ability of PLA chains to crystallize. These results are quite in

Table II. Transition Temperatures and Degree of Crystallinity of "0-day" Blends Measured by DSC

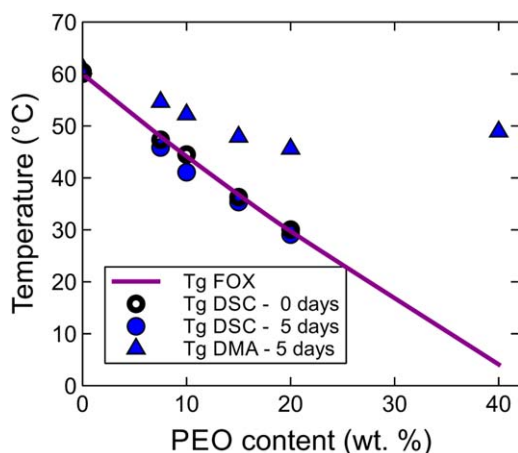| Samples designation	T_g (°C)	T_c (°C)	T_f (°C)	$X_{c\ PLA}$ (%)
PLA	60	108	168	0
PLA10PEO	44	82	166	5
PLA10PEO3MMT	47	83	167	7
PLA15PEO	36	77	166	8
PLA15PEO3MMT	38	78	167	8
PLA20PEO	30	71	166	9
PLA20PEO3MMT	31	71	167	16

Figure 2. Dependence of experimental (symbols) and theoretical (line) T_g values on PEO content. [Color figure can be viewed in the online issue, which is available at wileyonlinelibrary.com.]

agreement with Nakafuku et al. who have shown that PEO addition in PLA/PEO blends enables PLA chains crystallization from the melt, contrary to neat PLA. According to the authors, PEO chains in the liquid state act as a lubricant and hence have a so-called "diluent effect" in the PLA crystallization in the binary blends.[31] Figure 3 also supports that PEO cannot crystallize when its proportion is limited to 20 wt % or less in agreement with the DSC traces (Figure 1).

When PEO weight fraction is higher than 20%, both DSC and XRD traces suggest that PEO crystallizes and its degree of crystallinity increases with PEO content (Figures 1 and 2). On one hand, DSC traces show a melting peak corresponding to PEO crystalline phase (55–60°C) and PEO crystallinity rate calculated from this peak increases with PEO fraction (Figure 1). On the other hand, two crystalline peaks appear at 22.2° and 27.1° ($d = 4.6$ and 3.8 Å, respectively). Their intensity increases as well with PEO content (Figure 3).

All the results obtained on binary PLA/PEO blends thus tend to demonstrate that the miscibility limit of PEO in PLA is around 20 wt %. Consequently, in order to maximize both PLA use
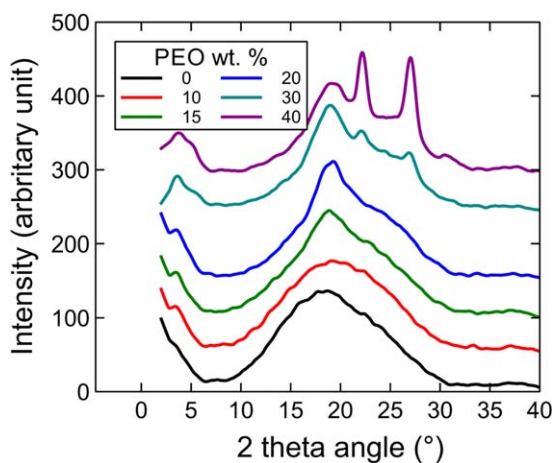
and plasticizing effects of PEO, the study carried out on PLA/PEO/clay ternary blends reported below has been limited to PEO concentrations up to 20 wt %.

Structure of PLA/PEO/Clay Ternary Blends

Small angle scattering patterns of the PLA/PEO/clay ternary blends are reported in Figure 4. All of them are characterized by a single diffraction peak in the low angle region, generally attributed to the basal spacing of clay tactoids. The measured basal spacing for all the nanocomposites is around 6 Å higher than the basal spacing determined for the native clay.

Therefore, the composite structure of the ternary blends is mainly intercalated at a nanometric scale, whereas PLA/unmodified clay blends reported in the literature so far are microcomposites.[4,12] The intercalation state obtained for the ternary blends is actually very similar to the intercalation state of intermediate PEO/MMT masterbatches compounded during the first extrusion step. To illustrate this, the diffraction peak of the PEO/17.5%MMT masterbatch used in the preparation of the PLA15PEO3MMT sample is also presented in Figure 4. Accordingly, the XRD analysis suggest that the intercalated structure revealed in the ternary blends is mostly related to the confinement of PEO chains in the interlayer spacings as obtained during the masterbatch compounding.

As shown in Figure 5, T_g of the 0-day ternaries are greater than T_g of the binary counterparts. Therefore DSC analysis suggests that, for a given PEO/polymer ratio, PLA chains have a little less mobility in the ternary blends containing clay. This trend appears more pronounced for blends containing less PEO, i.e., for ternary blends derived from masterbatches having higher clay content (Figure 5). Presumably PEO chains are more intercalated when clay content is higher in the masterbatch. In these blends, less PEO chains would be available to plasticize PLA as the number of PEO chains preliminarily confined increase. This assumption is in accordance with the hypothesis that PEO chains dispersion obtained after the PEO/clay extrusion is maintained in the final ternary blends. The study carried out by Paul et al on plasticized and nonplasticized clay-based composites
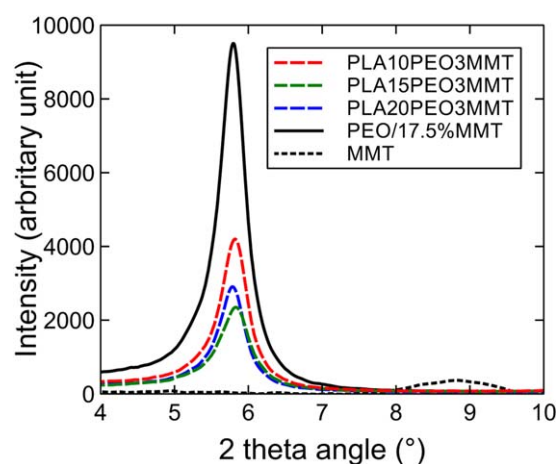

Figure 3. XRD spectra of PLA/PEO binary blends. [Color figure can be viewed in the online issue, which is available at wileyonlinelibrary.com.]

Figure 4. XRD spectra of MMT (clay), PEO/17.5%MMT masterbatch and ternaries. [Color figure can be viewed in the online issue, which is available at wileyonlinelibrary.com.]
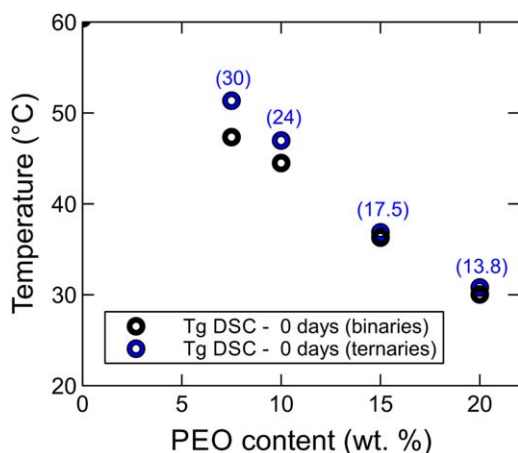
Figure 5. Dependence of "0-day" measured T_g values on PEO content. Masterbatch clay fraction used is shown into brackets for each ternary. [Color figure can be viewed in the online issue, which is available at wileyonlinelibrary.com.]

suggests a competition between PLA and PEG chains for the intercalation. No intercalation was detected for the PLA/Cloisite®Na+ composites, whereas its plasticized counterpart was characterized by an increase of the interlayer distance similar to this study (ca. 6Å). The authors noticed also that T_g of the nanocomposite is higher than the binary counterpart and that the intercalation height does not change by increasing clay concentration up to 10%. They concluded to the selective intercalation of PEG chains in the considered PLA/PEG/clay ternary blend.[12]

Ageing of PLA/PEO/Clay Ternary Blends and Effect of Unmodified Clay

Thermal Behavior of Binary and Ternary Blends. Typical DSC curves of 0-day samples and samples aged up to 220 days are shown in Figure 6. Corresponding transition temperatures and crystallinity degree values are summarized in Table III. The thermograms change with ageing time for all studied blends.

On one hand, moderate changes with ageing time are noticed for the PLA10PEO and PLA10PEO3MMT samples. The growth
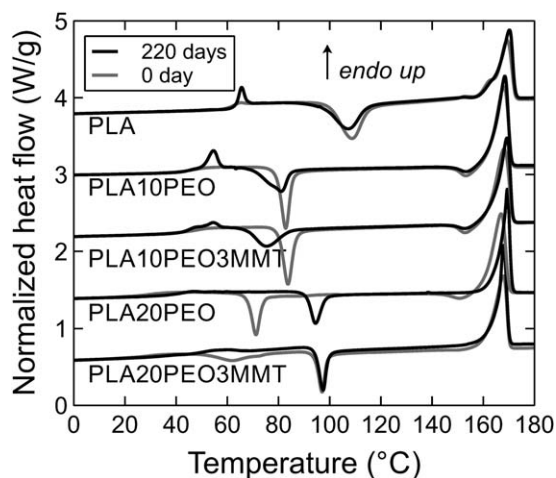

Figure 6. DSC curves of PLA and blends, "0-day" and 220-day aged samples.

Table III. Influence of Ageing Time on Transition Temperatures and Crystallinity Degree of PLA, Binary and Ternary Blends Measured by DSC

Ageing time (day)	$T_{g\ DSC}$ (°C)	T_{c1} (°C)	T_{c2} (°C)	$\Delta Hf_{\alpha'-\alpha}$ (J/g)	$X_{c\ PLA}$ (%)
PLA					
0	60	108	x	n.d.	0
5	60	105	x	n.d.	0
120	61	105	x	n.d.	6
220	61	107	x	n.d.	4
PLA10PEO					
0	44	82	x	−3.4	5
5	41	80	x	−2.2	12
30	44	80	x	−1.4	11
120	n.d.	79	x	−2.3	18
220	46	81	x	−2.5	16
PLA15PEO					
0	36	77	x	−4.0	8
5	35	79	x	−0.2	22
30	37	x	91	−0.1	26
120	n.d.	x	91	x	29
220	41	x	94	x	24
PLA20PEO					
0	30	71	x	−2.8	9
5	29	x	90	x	15
30	40	x	90	x	18
120	n.d.	x	92	x	26
220	39	x	94	x	22
PLA10PEO3MMT					
0	47	83	x	−3.8	7
5	42	79	x	−3.5	10
30	41	79	x	−2.1	8
120	n.d.	76	x	−2	17
220	44	75	x	−2	17
PLA15PEO3MMT					
0	38	78	x	−3.8	13
5	36	75	x	−0.6	20
30	39	77	89	−0.4	18
120	n.d.	x	92	x	23
220	42	x	95	x	17
PLA20PEO3MMT					
0	31	71	x	−2.5	16
5	40	x	92	x	24
30	39	x	92	x	16
120	n.d.	x	95	x	28
220	n.d.	x	97	x	23

of a moderate endothermic peak just after the glass transition is mainly noticed (Figure 6). This peak is characteristic of the relaxation of locally ordered domains formed as part of the PLA chains physical ageing.[19,21] In particular, the enthalpy measured for the binary blends after 220 days ageing is nearly 2 times
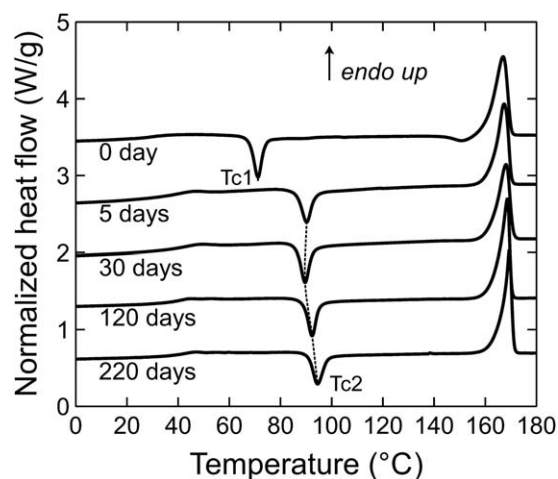
Figure 7. DSC curve evolution with ageing time for binary blend PLA20PEO.

higher than the value measured for PLA. This probably originates from the mobility enhancement of PLA chains in the PLA10PEO sample, which enables them to reorder easier and faster. Interestingly, the enthalpy value measured for the PLA10-PEO3MMT ternary after 220 days is the fourth of the one determined for the PLA10PEO binary. In addition to the endothermic peak evolution, T_g slightly increases over the observation period for PLA and binaries and ternaries containing 10 wt % of PEO. The overall increase is however slightly weaker in presence of clay. Also, changes occurring in the T_c region for the PLA10PEO and PLA10PEO3MMT samples are minor. In fact, initially, the cold-crystallization corresponding to PLA is observed at a lower temperature (T_{c1}) (Figure 1). No variation of T_{c1} is observed over time for the binary. T_{c1} measured for the ternary slightly decreases (Table III).

On the other hand, for the blends containing 20 wt % of PEO, the changes detected in the thermograms with ageing time are different and much more significant. T_g increases rapidly by around 10°C over the ageing period (Table III) while no endothermic peak appears. At the same time, after only 5 days, the cold-crystallization peak appears significantly shifted to higher temperature values compared to the 0-day thermograms. This can be considered as a fast transition from a cold-crystallization at low temperature (T_{c1}, ~70°C) to a cold-crystallization at higher temperature (T_{c2}, ~90°C) (Figure 7, Table III). This T_{c1}–T_{c2} transition suggests a fast loss of mobility for PLA chains, probably associated to rapid phase segregation between PLA and PEO in the amorphous phase. Afterward, T_{c2} continues to increase slowly indicating that ageing is still going on after 220 days. Regarding the ternary PLA20PEO3MMT, no influence of the clay on the T_{c1}–T_{c2} transition is clearly revealed.

In between, the blends containing 15 wt % of PEO stand as intermediate cases in terms of ageing behavior and kinetics (Figure 8, Table III). Indeed, the noticed T_g increase over time is more moderate in that case than for samples containing more PEO, and it seems to combine the growth of an endothermic peak in the T_g region and the T_{c1}–T_{c2} transition observed for

the PLA20PEO blend. The kinetics of this latter transition is also slower, lower plasticizer content resulting in lower chains mobility. Specifically the cold-crystallization peak centered on T_{c2} starts to develop over time while the peak centered on T_{c1} tends to disappear but does not completely vanish. Here a progressive loss of mobility for PLA chains over time is suggested, the ageing being such that two PLA phases with significantly different mobility coexists in the material over a period. The amorphous phase associated to T_{c2} is presumably poorer in PEO and hence called PLA-rich phase.[15,16] The observed T_{c1}–T_{c2} transition indicates that the PLA-rich phase becomes more predominant over time, and this at the expense of the initial PLA/PEO phase as T_{c1} and T_{c2} peak amplitudes respectively fade and increase. The presence of a double cold-crystallization peak is observed after 19 days ageing in the case of the binary PLA15PEO and after 34 days in the case of the ternary PLA15-PEO3MMT. At this latter time only T_{c2} appears for the binary blend. T_{c1}–T_{c2} transition therefore occurs later for the ternary blend. Besides, a slow increase of T_{c2} after the transition is again observed irrespective of the presence of clay. Thus the PLA rich-phase formed keeps getting richer in PLA over time even after 220 days, and hence the suggested deplasticization carries on.

Moreover, T_{c1}–T_{c2} transition observed for blends made of 15 and 20 wt % of PEO is very closely associated to the progressive disappearance of the exothermic peak immediately preceding the main melting peak. This exothermic peak corresponds to α' crystals fusion-recrystallization into more ordered α crystals.[17,19] The associated values of exothermic enthalpy ($\Delta H_{\alpha'-\alpha}$) are reported in Table III. This tends to demonstrate the presence of α-form crystals only after the cold-crystallization at higher temperature (T_{c2}, ~90°C), whereas cold-crystallization of plasticized PLA chains at lower temperature (T_{c1}, ~70°C) produces, at least partly, α'-form crystals. As part of their binary blends ageing, Jia et al. noticed the decrease of $|\Delta H_{\alpha'-\alpha}|$ as well. Their results suggested that PLA cold-crystallization occurs over the ageing period. Regarding the observed $|\Delta H_{\alpha'-\alpha}|$ decrease, it was supposed that the involved slow cold-crystallization induced chain rearrangements.[13] However for our binary and ternary
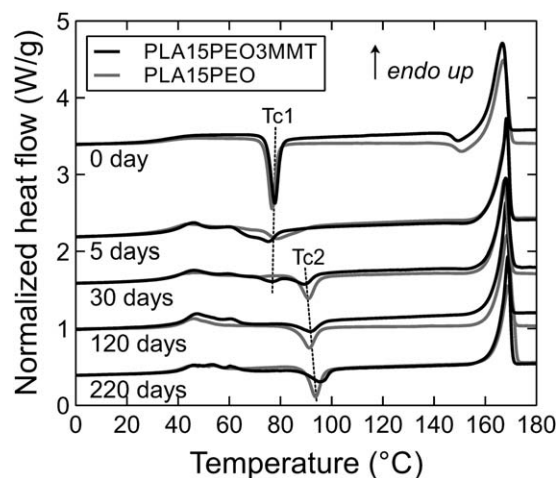

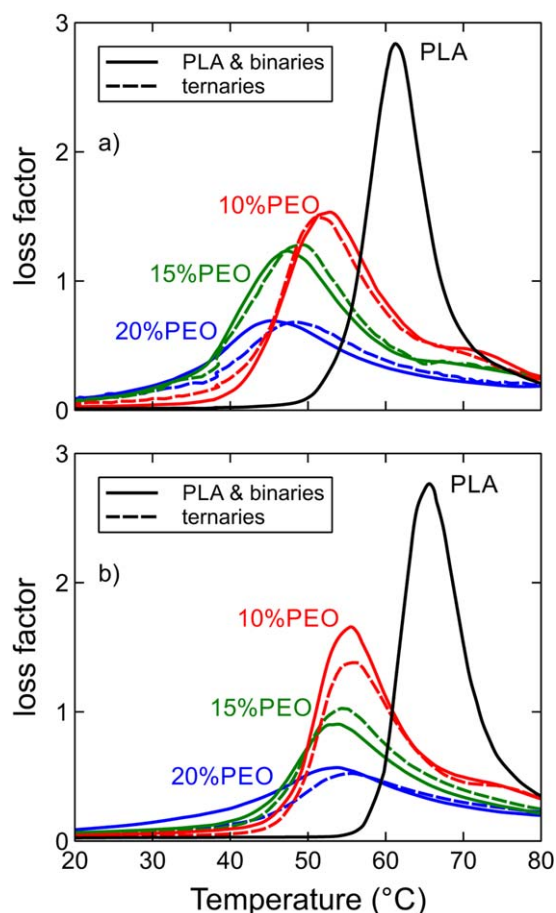**Figure 8.** DSC curves evolution with ageing time for PLA15PEO and PLA15PEO3MMT sample.

Figure 9. DMA Loss factor—tan(δ)—as a function of temperature for (a) 5-day aged and (b) 120-day aged binary and ternary blends samples. [Color figure can be viewed in the online issue, which is available at wileyonlinelibrary.com.]

Figure 10. Storage modulus—E'—as a function of temperature for (a) 5-day aged and (b) 120-day aged binary and ternary blends samples. [Color figure can be viewed in the online issue, which is available at wileyonlinelibrary.com.]

Finally, by analyzing the loss factor traces at low temperatures, secondary maximums are visible at $-52°C$ and $-53°C$, respectively for PLA15PEO and PLA15PEO3MMT samples aged 60 days (Figure 11). These temperatures are relatively close to the neat PEO $T_{g \text{ DMA}}$ value ($-46°C$). Therefore, it confirms the formation of a PEO phase upon ageing, and hence the phase separation suggested by the DSC results.

blends, no crystalline rearrangements have been detected by wide-angle X-ray scattering measurements carried out over time (not reported here). Interestingly, the slower $T_{c1}-T_{c2}$ transition observed for the PLA15PEO3MMT sample is associated to a slightly slower decrease of $|\Delta H_{\alpha'-\alpha}|$ compared to the PLA15PEO sample.

Viscoelastic Behavior of Binary and Ternary Blends. Loss factors traces of samples aged 5 and 120 days are shown in Figure 9. An increase of $T_{g\text{DMA}}$ over the 115 days period is observed for all references. Besides, the higher the PEO weight fraction, the more pronounced the rise. In agreement with DSC measurements, all the references undergo ageing phenomena resulting in a progressive T_g rise, being more significant for blends containing more PEO.

The traces of the storage modulus (E') as a function of temperature of the same samples are depicted in Figure 10. After α relaxation corresponding to the glass transition, the subsequent rise of E' at higher temperatures is related to the cold-crystallization of the material. DMA results confirm the $T_{c1}-T_{c2}$ transition for blends containing 15 and 20 wt % of PEO after, respectively, a few days ageing and 120 days ageing.
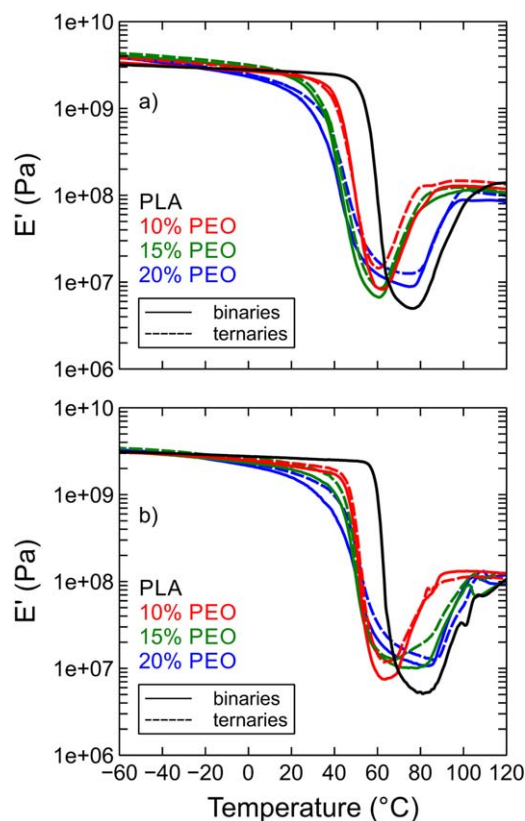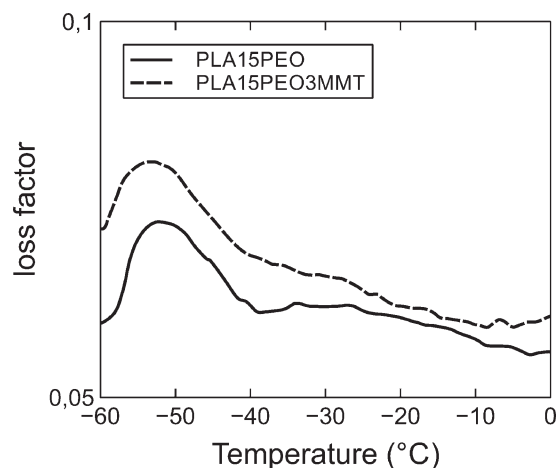

Figure 11. DMA loss factor—tan(δ)—as a function of temperature for 60-day aged PLA15PEO and PLA15PEO3MMT samples.

CONCLUSIONS

Poly(lactic acid) (PLA), poly(ethylene oxide) (PEO) and unmodified clay were compounded in order to investigate the ageing of ternary blends under ambient conditions. A master-batch route was used to overcome as much as possible the poor affinity between PLA and clay. Hydrophilic PEO and clay were first melt-blended before diluting the produced masterbatches into PLA during a second extrusion.

Firstly, in the PLA/PEO binary blends taken as references, PEO is fully miscible with PLA up to 20 wt %. In the ternary blends, the intercalated structure formed during masterbatch processing is maintained attesting of the good affinity between PEO and unmodified clay. Because of the presence of clay, part of the PEO plasticization potential is lost in the ternary blends compared to binary blends. It confirms the strong interactions existing between PEO and clay.

The thermal behavior of the blends was also analyzed as a function of time to evidence the structural evolution of the blends upon ageing, and two distinct phenomena were revealed: (a) the growth of an endothermic relaxation associated to the physical ageing of PLA chains and (b) a cold-crystallization temperature (T_c) transition to a higher value due to a mobility change related to PLA/PEO phase segregation. The relative importance of these two events primarily depends on PEO content. Over the 220-day observation period, only physical ageing occurs in samples containing 10 wt % or less of PEO whereas sole T_c transition affects blends close to the miscibility limit. In between, 15 wt % PEO blends stand as an intermediate case combining both phenomena. How fast thermal response changes intervene depends also on the presence of unmodified clay. This latter appears to limit PLA physical ageing and slow down PLA/PEO phase segregation in the PLA/PEO/clay ternary blends. Moreover, dynamic mechanical analysis confirms the segregation, aged blends being characterized by the presence of a PEO T_g.

ACKNOWLEDGMENTS

REFERENCES

1. Rodriguez-Llamazares, S.; Rivas, L. B.; Pérez, M.; Perrin-Sarazin, F. *High Perf. Polym.* **2012**, *24*, 254.

2. Ozkoc, G.; Kemaloglu, S. *J. Appl. Polym. Sci.* **2009**, *114*, 2481.

3. Tanoue, S.; Hasook, A.; Lemoto, Y.; Unryu, T. *Polym. Compos.* **2006**, *27*, 256.

4. Shibata, M.; Someya, Y.; Orihara, M.; Miyoshi, M. *J. Appl. Polym. Sci.* **2006**, *99*, 2594.

5. Scatto, M.; Salmini, E.; Castiello, S.; Coltelli, M.-B.; Conzatti, L.; Stagnaro, P.; Andreotti, L.; Bronco, S. *J. Appl. Polym. Sci.* **2013**, *127*, 4947.

6. Martino, V. P.; Jiménez, A.; Ruseckaite, R. A.; Avérous, L. *Polym. Adv. Technol.* **2011**, *22*, 2206.

7. Strange, M.; Plackett, D.; Kaasgaard, M.; Krebs, F. C. *Solar Energy Mater. Solar Cells* **2008**, *92*, 805.

8. Ahmed, J.; Varshney, S. K.; Auras, R.; Hwang, S. W. *J. Food Sci.* **2010**, *75*, N97.

9. Thellen, C.; Orroth, C.; Froio, D.; Ziegler, D.; Lucciarini, J.; Farrell, R.; D'Souza, N. A.; Ratto, J. A. *Polymer* **2005**, *46*, 11716.

10. Soulestin, J.; Prashantha, K.; Lacrampe, M.-F.; Krawczak, P. In Handbook of Bioplastics and Biocomposites Engineering Applications; Pilla, S., Ed.; Wiley-Scrinever: USA, **2011**; Chapter 4, p 77.

11. Ray, S. S.; Maiti, P.; Okamoto, M.; Yamada, K.; Ueda, K. *Macromolecules* **2002**, *35*, 3104.

12. Paul, M.-A.; Alexandre, M.; Degée, P.; Henrist, C.; Rulmont, A.; Dubois, P. *Polymer* **2003**, *44*, 443.

13. Jia, Z.; Tan, J.; Han, C.; Yang, Y.; Dong, L. *J. Appl. Polym. Sci.* **2009**, *114*, 1105.

14. Pluta, M.; Paul, M.-A.; Alexandre, M.; Dubois, P. *J. Polym. Sci. B Polym. Phys.* **2006**, *44*, 312.

15. Hu, Y.; Hu, Y. S.; Topolkaraev, V.; Hiltner, A.; Baer, E. *Polymer* **2003**, *44*, 5681.

16. Hu, Y.; Hu, Y. S.; Topolkaraev, V.; Hiltner, A.; Baer, E. *Polymer* **2003**, *44*, 5711.

17. Martino, V. P.; Ruseckaite, R. A.; Jiménez, A. *Polym. Int.* **2009**, *58*, 437.

18. Martino, V. P.; Ruseckaite, R. A.; Jiménez, A.; Averous, L. *Macromol. Mater. Eng.* **2010**, *295*, 551.

19. Burgos, N.; Martino, V. P.; Jiménez, A. *Polym. Degrad. Stab.* **2013**, *98*, 651.

20. Rasal, R. M.; Janorkar, A. V.; Hirt, D. E. *Progr. Polym. Sci.* **2010**, *35*, 338.

21. Celli, A.; Scandola, M. *Polymer* **1992**, *33*, 2699.

22. Pan, P.; Zhu, B.; Dong, T.; Yazawa, K.; Shimizu, T.; Tansho, M.; Inoue, Y. *J. Chem. Phys.* **2008**, *129*, 184902–1–10.

23. Ljungberg, N.; Wesslén, B. *Biomacromolecules* **2005**, *6*, 1789.

24. Ljungberg, N.; Wesslén, B. *J. Appl. Polym. Sci.* **2004**, *94*, 2140.

25. Ljungberg, N.; Colombini, D.; Wesslén, B. *J. Appl. Polym. Sci.* **2005**, *96*, 992.

26. Ljungberg, N.; Wesslén, B. *J. Appl. Polym. Sci.* **2003**, *88*, 3239.

27. Ljungberg, N.; Wesslén, B. *Polymer* **2003**, *44*, 7679.

28. Gumus, S.; Ozkoc, G.; Aytac, A. *J. Appl. Polym. Sci.* **2012**, *123*, 2837.

29. Nijenhuis, A. J.; Colstee, E.; Grijpma, D. W. *Polymer* **1996**, *37*, 5849.

30. Vaia, R. A.; Vasudevan, S. *Adv. Mater.* **1995**, *7*, 154.

31. Nakafuku, C. *Polymer* **1996**, *28*, 568.